

Article

A Transaction Model and Profit Allocation Method of Multiple Energy Storage Oriented to Versatile Regulation Demand

Jin Zhi ¹, Yuantian Xue ¹, Xiaozhu Li ², Changcheng Song ¹, Kaipeng Zhang ¹ and Laijun Chen ^{2,*}

¹ State Grid Gansu Electric Power Company, Wuwei Power Supply Company, Wuwei 733000, China; jin_zhi@163.com (J.Z.); yuantian_xue@163.com (Y.X.); changcheng_song@163.com (C.S.); kaipeng_zhang@163.com (K.Z.)

² Department of Electrical Engineering, Tsinghua University, Beijing 100190, China; lixiaozhu@tsinghua.edu.cn

* Correspondence: chenlaijun@tsinghua.edu.cn

Abstract: This study proposes a day-ahead transaction model that combines multiple energy storage systems (ESS), including a hydrogen storage system (HSS), battery energy storage system (BESS), and compressed air energy storage (CAES). It is catering to the trend of a diversified power market to respond to the constraints from the insufficient flexibility of a high-proportion renewable energy system (RES). The model is a double-layer game based on the Nash–Stackelberg–cooperative (N–S–C) game. Multiple users in the upper layer form the Nash game with the goal of maximizing their own benefits, while the multiple ESSs in the lower layer form a cooperative game with the goal of maximizing the overall benefits; the two layers form a Stackelberg game. Moreover, an allocation mechanism is proposed to balance the overall and individual rationality and promote the sustainable development of multiple ESSs, considering the operational characteristics. A numerical simulation is carried out using the rationality and effectiveness of the proposed model, which is based on data from the renewable energy gathering area in northwest China. The results show that this strategy shortens the energy storage payback period and improves the energy storage utilization. The simulation results indicate that small-scale energy storage with a rated power of less than 18 MWh does not have a price advantage, indicating the need to improve the configuration capacity of energy storage in the future from decentralized energy storage to independent/shared energy storage.

Keywords: versatile regulation demand; multiple energy storage; transaction mode; profit allocation; engineering game theory



check for updates

Citation: Zhi, J.; Xue, Y.; Li, X.; Song, C.; Zhang, K.; Chen, L. A Transaction Model and Profit Allocation Method of Multiple Energy Storage Oriented to Versatile Regulation Demand.

Sustainability **2023**, *15*, 15849.

<https://doi.org/10.3390/su152215849>

Academic Editor: Pablo García Triviño

Received: 18 September 2023

Revised: 28 October 2023

Accepted: 2 November 2023

Published: 11 November 2023



Copyright: © 2023 by the authors. Licensee MDPI, Basel, Switzerland. This article is an open access article distributed under the terms and conditions of the Creative Commons Attribution (CC BY) license (<https://creativecommons.org/licenses/by/4.0/>).

1. Introduction

Due to the rapid development of new power systems (RES), there is an urgent need to meet the demand for backup capacity, peaking, frequency regulation (FR), and other multiregulation requirements [1]. The HSS, CAES, and BESS have a competitive edge as a flexible regulation resource in versatile scenarios [2]. However, the ESS faces development bottlenecks with low energy utilization and long payback periods [3]. In May 2022, the National Energy Administration of China issued a notice on further promoting the participation of a new type of ESS in the electricity market and scheduling application, encouraging the ESS to optimize scheduling and participate in the power market to improve cost-effectiveness [4]. It can be a response to the challenges of the insufficient flexibility of a high-proportion RES in an efficient and economical market transaction model with the participation of multiple ESSs that meet various regulatory demands.

The multiple energy storage system can overcome the constraints of the poor flexibility in a single energy storage system based on the characteristics for complementary differences in response and by reducing the mismatch between supply and different time scale demands [5]. Ref. [6] proposed a multi-timescale (before and during the day) coordinated optimization method for an energy hub with multienergy flow and multiple

ESSs for the short-term scale with multiadjustment requirements. Ref. [7] constructed a rolling optimization method for a user-side ESS operation allocation for the intraday and the month-ahead. Tatsuya et al. constructed a model of a grid-connected photovoltaic (PV) renewable generation station (RGS) incorporating the HSS by [8], which analyses the intercoupling between different PV capacities, the system cost, and greenhouse effect gas emissions, showing that the HSS has the economic advantage of an ESS for long periods of time. A mixed-integer linear programming model for the long- and short-term synergistic operation of the HSS and BESS was constructed in [9], which deals with the response characteristics of multiple ESSs and significantly reduces the cost of an HSS compared to a single ESS. Ref. [10] explored the role of a long-term ESS in supporting the reliable operation of an RES and compared the operational characteristics of multiple ESSs. The necessity, feasibility, and economics of an HSS participating in the long-term scale under the operation of the RES have been studied. Yet, the existing multitype ESS cooperation strategy only considers the ESS operation and operating characteristics without considering the response cost of each type of ESS. Furthermore, achieving the maximum operational cost-effectiveness for an ESS to promote the sustainable development of multiple ESSs appears to be challenging.

The tremendous potential of multitype ESSs in the face of a multiscenario demand strongly promotes participation in market transactions to improve economic efficiency. ESSs mainly engage in multielectricity markets as a single entity, with the transaction mechanism categorized into independent and joint management [11]. Joint management can achieve the maximization of social benefits. Ref. [12] introduced composite operators to provide hydrogen, oxygen, and electricity storage services that operate in cooperative gaming with prosumers to minimize social costs. The participation of multitype ESSs in energy hubs for multi-timescale coordinated optimization was advised to meet integrated energy system peaking and track output planning needs in [13]. Ref. [14] proposed the multiobjective optimal scheduling for multiple ESSs, considering the overall system consumption and power fluctuation. Ref. [15] built a hybrid BESS and HSS, where the operator trades with the prosumers in the form of energy and capacity, sharing to incentivize the willingness of both to participate. Ref. [16] structured a hybrid ESS involving a BESS and HSS to eliminate system uncertainty and transfer seasonal energy. However, the ESS's heterogeneous economic characteristics, services provided, and objects faced are diversifying with the future evolution of the power grid [17], and participation in the market tends to be varied. The complex coupling relationship has led to the difficulty of clarifying the interaction between multiple participants, making it urgent to design a trading mechanism that balances the individual interest with the overall economic benefits.

Given these gaps, this study proposes a day-ahead trading pattern with multitype ESSs that are cooperative in the background of a high percentage of RESs to fulfil the multiscenario demands of RGSs. The main contributions of this study are summarized below:

- (1) We have constructed a multitype ESS containing an HSS, BESS, and CAES to satisfy the demands of multiscenarios for standby, peak shaving, and FR. The multitype ESS, compared to a traditional single ESS, has different response characteristics, resolving the issue of poor flexibility in the power market.
- (2) We have proposed a two-layer game model of the N–S–C game, balancing the total cost of regulation and the profit of multitype, independent operating. The game pattern, in contrast to the Stackelberg game model, addresses a trading model where multiple ESS users participate independently with multiple ESSs, which conforms to the transaction mode of the multitype ESS operating as an independent entity.
- (3) We have designed a value allocation strategy based on the operating characteristics of multitype ESSs, utilizing the average regulation cost and FR mileage factor to determine the benefit allocation. The new strategy, which deviates from the Shapley value method, efficiently clarifies the actual contribution of multitype ESSs, acknowledging the balance between the overall rationality and individual rationality.

2. Day-Ahead Trading Framework of a Multitype ESS Collaboration

The overall framework of day-ahead trading for the multitype ESS collaboration is shown in Figure 1. The framework includes multiple ESS users and multiple ESSs. The framework is given below:

- (1) Multiple RGSs and power grids, as multiple ESS users, send adjustment requirements to multiple ESSs according to the power generation and net load curves.
- (2) The multiple ESSs include a HSS, ESS, and CAES with different response characteristics, which participate in electricity trading as independent operators. The energy storage operator (ESO) centralizes regulation and unifies the management of multiple operating entities. The multiple ESSs return the auxiliary service price to the ESS user according to the ESS operation and the adjustment cost in order to respond to the needs of users. The framework can also balance the interests of multiple ESS entities by considering the characteristics of multiple ESSs to develop a value allocation strategy.

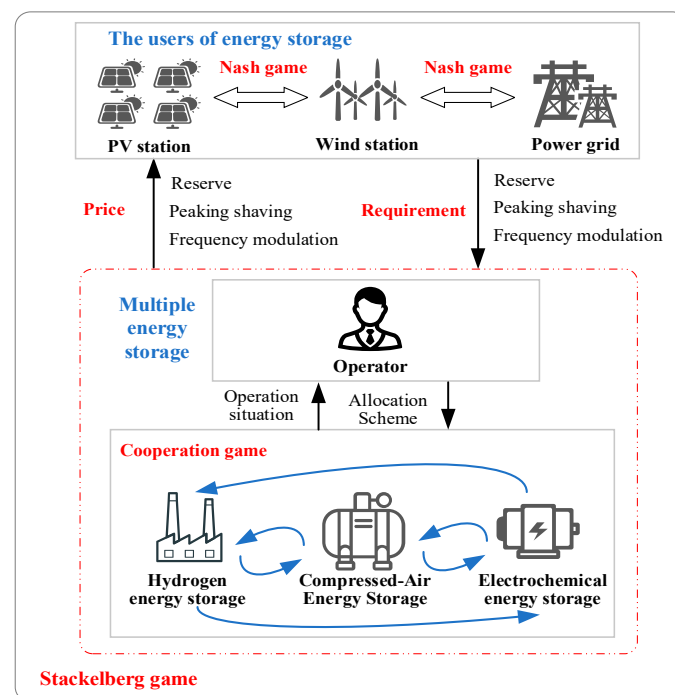


Figure 1. Framework of the collaboration of multiple ESSs for day-ahead joint trading.

In the day-ahead joint trading, the players contain a wind/photovoltaic generation station, RGSs, ESSs, and power grids. The demand for ESS regulation, wind, or photovoltaic power curtailment and thermal power unit output make plans using competition for players in the day-before trading. There are the following regulations:

- (1) Multiple ESS entities that meet the trading access conditions upload various types of regulatory demand response plans and service prices to the ESO according to the relevant operational constraints, maintenance, and life loss costs with the goal of maximizing the overall benefit of multiple ESSs.
- (2) ESOs release value distribution plans to ESS entities to balance the interests of each entity based on the difference in response characteristics of multiple ESSs.

During the above process, ESS users make decisions to maximize their own benefits and submit their demands to multiple ESSs. The Nash game is formed among all ESS users. Subsequently, the multiple ESSs make decisions to formulate various demand service prices and internal value distribution schemes to maximize the overall income. Therefore, a cooperative game is formed among multiple ESS entities. The Stackelberg game is formed between ESS users and multiple ESSs. Participants cannot increase benefits or reduce costs by unilaterally changing their own strategies after the market equilibrium is reached.

The day-ahead trading organization patterns of a multiple ESS collaboration is as follows:

Step 1: ESS users, such as RGSs (wind power or photovoltaic) and power grids, can obtain the amount of wind/photovoltaic power curtailment ($P_t^{W_loss}, P_t^{PV_loss}$), the output plan of thermal power units ($P_{i,t}^G, i \in N_G$), and the demand for ESS utilization ($P_t^{RV}, P_t^{PS}, P_t^{PFR}$) through the Nash game.

Step 2: Each ESS entity declares the cost of standby power, peak shaving, FR ($C_k^m, k \in \{Hy, El, Aa\}, m \in \{B, PS, PFR\}$), and electric energy ($P_k^m, k \in \{Hy, El, Aa\}, m \in \{B, PS, PFR\}$) to the ESO, where Hy, El, and Aa are HSS, BESS, and CAES, respectively. B, PS, and PFR are defined as standby, peaking, and FR regulation requirements, respectively.

Step 3: ESOs make decisions through cooperative gaming, while feeding back the response results ($P_t^{RV*}, P_t^{PS*}, P_t^{PFR*}$) and transaction prices ($\zeta_t^{RV}, \zeta_t^{PS}, \zeta_t^{PFR}$) of each type of regulated demand to multiple ESS users.

Step 4: Return to Step 1. The energy storage user adjusts the demand for each type for more energy storage regulation, wind/photovoltaic power curtailment, and the thermal power unit output plan until the trading process reaches equilibrium. That means the declared amount, the trading price, and the thermal power unit output plan no longer change.

3. Results

3.1. Basic Assumptions of the Model

The day-ahead trading model of the multiple ESS coordination has the following assumptions:

- (1) The load is an inflexible load.
- (2) The power generation cost of the thermal power unit is a quadratic function of output, FR, and standby capacity cost become linear functions of output [18].
- (3) The ESS capacity, FR, and reserve cost are all linear functions of the charge and discharge capacity.
- (4) The declared amount of FR mileage and standby capacity of each ESS owner or thermal unit takes into account both upward/downward FR and standby situations.

The N-S-C game is constituted with multiple ESS users in a day-ahead market transaction in which multiple ESSs collaboratively participates, as described in the analysis of Section 2:

3.2. Multitype User Demand Decision-Making Based on the Nash Game

The objective is satisfying both the maximum benefit of each ESS user and the minimum feedback deviation. The optimal benefit of the wind and PV farms is equated to the minimum cost of the wind/PV curtailment, and the optimal benefit of the grid is equated to the minimum cost of the regulation of the thermal power units.

- (1) Benefit of the new energy station ($U_{W/PV}$)

$$U_{W/PV} = \sum_t^T \zeta_t^{W/PV_loss} P_t^{W/PV_loss} \quad (1)$$

- (2) Power grid benefit (U_{Grid})

$$U_{Grid} = \sum_t^T \sum_i^{N_G} \left[f^B(P_{i,t}^G) + f^{PFR}(P_{i,t}^{G_PFR}) + f^{RV}(Q_{i,t}^{G_RV}) \right] \quad (2)$$

- (3) Feedback deflection (U_{Dev})

$$U_{Dev} = \sum_t^T \left[\zeta_{Dev}^{PS} (P_t^{PS} - P_t^{PS*})^2 + \zeta_{Dev}^{PFR} (P_t^{PFR} - P_t^{PFR*})^2 + \zeta_{Dev}^{RV} (P_t^{RV} - P_t^{RV*})^2 \right] \quad (3)$$

The above optimization problem is described as:

$$obj. \min_{P_t^{PS}, P_t^{PFR}, P_t^{PV}} U_i, i \in \{W, PV, Grid, Dev\}, \forall i \quad (4)$$

$$s.t. \sum_{i=1}^{N_G} P_{i,t}^G + P_t^{PS} + P_t^W - P_t^{W_loss} + P_t^{PV} - P_t^{PV_loss} = D_t, \forall t \quad (5)$$

$$\sum_{i=1}^{N_G} P_{i,t}^{G_PFR} + P_t^{PFR} \geq \eta^{PFR} (D_t - P_t^W - P_t^{PV}), \forall t \quad (6)$$

$$\left(\sum_{i=1}^{N_G} P_{i,t}^{G_PFR} + P_t^{PFR} \right) + \left(\sum_{i=1}^{N_G} Q_{i,t}^{G_RV} + P_t^{RV} \right) \geq \eta^{RV} (P_t^W + P_t^{PV}) + \eta^{PFR} (D_t - P_t^W - P_t^{PV}), \forall t \quad (7)$$

$$P_{i,t}^G + P_{i,t}^{G_PFR} + Q_{i,t}^{G_RV} \leq P_{i,max}^G, \forall i, t \quad (8)$$

$$P_{i,t}^G + P_{i,t}^{G_PFR} + Q_{i,t}^{G_RV} \leq P_{i,min}^G, \forall i, t \quad (9)$$

$$0 \leq P_{i,t}^{G-\alpha} \leq P_{i,max}^{G-\alpha}, \alpha \in \{PFR, RV\}, \forall i, t \quad (10)$$

$$P_{i,t+1}^G + P_{i,t+1}^{G_PFR} + Q_{i,t+1}^{G_RV} - (P_{i,t}^G - P_{i,t}^{G_PFR} - Q_{i,t}^{G_RV}) \leq P_i^{RU}, \forall i, t \quad (11)$$

$$P_{i,t}^G + P_{i,t}^{G_PFR} + Q_{i,t}^{G_RV} - (P_{i,t+1}^G - P_{i,t+1}^{G_PFR} - Q_{i,t+1}^{G_RV}) \leq P_i^{RD}, \forall i, t \quad (12)$$

As shown in Equation (6), the balance of power constraints in Equations (7) and (8) are the FR and standby demand constraints, respectively. η^{PFR} and η^{RV} are the FR demand coefficients due to net load fluctuations and the standby demand coefficients due to the stochasticity of a new energy output. The FR power can be used as the standby capacity for the FR power surplus, and the price is low. In addition, the FR capacity replaces the standby capacity for the FR, and standby prices are equal [19]. Equations (6)–(10) represent the thermal unit output, upper and lower FR, and up and down reserve capacity plan constraints. The climbing constraints for the thermal units are represented by Equations (11) and (12).

3.3. Price Decision of Multitype Energy Storage Service Based on a Cooperative Game

Multiple ESSs use operators to make decisions through cooperative games, and the objective function is to maximize the overall revenue of the ESS. ESS operator revenues come with participation in ancillary services such as peaking, FR, and standby, as indicated below:

$$obj. \max_{P_t^{PS*}, P_t^{PFR*}, P_t^{PV*}, \zeta_t^{RV}, \zeta_t^{PS}, \zeta_t^{PFR}} U_{HES} = \zeta_t^{PS} (P_t^{ES_C} + P_t^{ES_D} + P_t^{ele} + P_t^{fue} + \mu_t^{AC} P_t^{AC} + \mu_t^{AC} P_t^{EX}) \\ + \zeta_t^{PFR} (P_t^{ES_PFR} + P_t^{HS_PFR} + P_t^{Aa_PFR}) + \zeta_t^{RV} (Q_t^{ES_RV} + Q_t^{HS_RV} + Q_t^{Aa_RV}) \quad (13)$$

There are the following constraints.

(1) BESS constraint

$$s.t. \begin{cases} 0 \leq P_t^{ES_C} \leq \mu_t^C P_{max}^{ES_C} \\ 0 \leq P_t^{ES_D} \leq \mu_t^D P_{max}^{ES_D} \\ \mu_t^C + \mu_t^D \leq 1 \end{cases}, \forall t \quad (14)$$

$$\begin{cases} 0 \leq P_t^{ES_PFR} \leq \omega^{ES_PFR} P_{max}^{ES_C} \\ 0 \leq Q_t^{ES_RV} \leq \omega^{ES_RV} Q_{max}^{ES_RV} \end{cases}, \forall t \quad (15)$$

$$\begin{cases} 0 \leq P_t^{ES_C} + P_t^{ES_PFR} + Q_t^{ES_RV} \leq P_{max}^{ES_C} \\ 0 \leq P_t^{ES_D} + P_t^{ES_PFR} + Q_t^{ES_RV} \leq P_{max}^{ES_D} \end{cases}, \forall t \quad (16)$$

$$\begin{cases} E_{\min}^{\text{ES}} \leq E_t^{\text{ES}} \leq E_{\max}^{\text{ES}} \\ E_t^{\text{ES}} = E_{t-1}^{\text{ES}} + \eta^{\text{ch}} \left(P_t^{\text{ES}_C} + P_t^{\text{ES}_PFR} + Q_t^{\text{ES}_RV} \right) - (1/\eta^{\text{dis}}) \left(P_t^{\text{ES}_D} + P_t^{\text{ES}_PFR} + Q_t^{\text{ES}_RV} \right), \forall t \end{cases} \quad (17)$$

$$E_0^{\text{ES}} = E_{23}^{\text{ES}} \quad (18)$$

The charging and discharging constraints of the BESS are described by Equation (14). Equations (15) and (16) are service response constraints for each type of BESS. Equation (17) is for the charge state constraints. In addition, Equation (18) aims to guarantee the sustainable operation of the ESS.

(2) HSS constraint

$$M_0^{\text{H}_2} = M_{23}^{\text{H}_2} \quad (19)$$

$$\begin{cases} M_{\min}^{\text{H}_2} \leq M_t^{\text{H}_2} \leq M_{\max}^{\text{H}_2} \\ M_t^{\text{H}_2} = M_{t-1}^{\text{H}_2} + \eta_{\text{ele}} P_t^{\text{ele}} - \frac{p_t^{\text{fue}}}{\eta_{\text{fue}}} \end{cases} \quad (20)$$

$$\begin{cases} P_t^{\text{ele}} + P_t^{\text{HS}_PFR} + Q_t^{\text{Aa}_RV} \leq Q^{\text{ele}} \\ P_t^{\text{fue}} + P_t^{\text{HS}_PFR} + Q_t^{\text{Aa}_RV} \leq Q^{\text{fue}} \end{cases} \quad (21)$$

$$0 \leq P_t^{\text{HS}_PFR} \leq \omega^{\text{HS}_PFR} Q^{\text{ele}} \quad (22)$$

Equation (19) is similar to Equation (8). The total HSS capacity of the tank should be less than the upper and lower limits, as shown in Equation (20). Equations (21) and (22) represent the service response constraints for each type of HSS.

(3) CAES constraint

$$\begin{cases} p_{\min}^{\text{st}} \leq p_t^{\text{st}} \leq p_{\max}^{\text{st}} \\ p_t^{\text{st}} = p_{t-1}^{\text{st}} + \left(\mu_t^{\text{AC}} \frac{R_g T_{\text{st},\text{in}}}{V_{\text{st}}} \dot{m}_{\text{AC},t} - \mu_t^{\text{EX}} \frac{R_g T_{\text{st}}}{V_{\text{st}}} \dot{m}_{\text{EX},t} \right) \end{cases} \quad (23)$$

$$\mu_t^{\text{AC}} + \mu_t^{\text{EX}} \leq 1, \forall t \quad (24)$$

$$\begin{cases} \mu_{t-1}^{\text{AC}} + \mu_t^{\text{AC}} - \mu_k^{\text{AC}} \leq 0, \forall i, t; t \leq k \leq T_{\text{on}}^{\text{AC}} + t - 1 \\ \mu_{t-1}^{\text{EX}} + \mu_t^{\text{EX}} - \mu_k^{\text{EX}} \leq 0, \forall i, t; t \leq k \leq T_{\text{on}}^{\text{EX}} + t - 1 \end{cases} \quad (25)$$

The constraint of the reservoir is represented by Equation (23), which is related to the air mass flow rate between the compression side and expansion side. The relationship between the expander power consumption and compressor work performed is shown in Equation (26). Equation (24) is the operating condition constraint. The minimum operating time constraint for the compression/expansion machine is represented by Equation (25).

$$\left(P_t^{\text{AC}} + P_t^{\text{Aa}_PFR} + Q_t^{\text{Aa}_RV} \right) \eta_{\text{AC}} = \dot{m}_{\text{AC},t} \frac{\gamma}{\gamma-1} R_g \cdot \left(\sum_{k=1}^{n-1} \left(T_{\text{AC},k,\text{in}} \left(\beta_{\text{AC},k}^{\frac{\gamma-1}{\gamma}} - 1 \right) + T_{\text{AC},n,t} \left(\beta_{\text{AC},n,t}^{\frac{\gamma-1}{\gamma}} - 1 \right) \right) \right) \quad (26)$$

$$\left(P_t^{\text{EX}} + P_t^{\text{Aa}_PFR} + Q_t^{\text{Aa}_RV} \right) = \eta_{\text{EX}} \dot{m}_{\text{EX},t} \frac{\gamma}{\gamma-1} R_g \cdot \sum_{j=1}^n \left(T_{\text{EX},j,\text{in},t} \left(1 - \beta_{\text{EX},k}^{-\frac{\gamma-1}{\gamma}} \right) \right) \quad (27)$$

(4) Multitype energy storage adjustment demand response constraints

$$\begin{cases} P_t^{\text{PS}*} = P_t^{\text{ES}_C} + P_t^{\text{ES}_D} + P_t^{\text{ele}} + P_t^{\text{fue}} + \mu_t^{\text{AC}} P_t^{\text{AC}} + \mu_t^{\text{AC}} P_t^{\text{EX}} \\ P_t^{\text{PFR}*} = P_t^{\text{ES}_PFR} + P_t^{\text{HS}_PFR} + P_t^{\text{Aa}_PFR} \\ P_t^{\text{RV}*} = Q_t^{\text{ES}_RV} + Q_t^{\text{HS}_RV} + Q_t^{\text{Aa}_RV} \end{cases} \quad (28)$$

3.4. Benefit Distribution Mechanism of Multitype Energy Storage Subjects

The Shapley allocation method can allocate the additional profit of the alliance according to the marginal contribution of each participant [20]. However, the interest of multiple ESSs is interactively coupled, which is related to the adjustment cost and response and cannot be completely decoupled. Therefore, it is necessary to improve the traditional Shapley allocation method. The distribution of benefits for each ESS subject is determined using the mean value of the regulation cost and the FR mileage factor of each storage system (the FR mileage factor of CAES is analysed to be one, according to Section 3.3). The improved Shapley allocation method is shown as follow:

$$C_B^{\text{ES}^*} = \frac{1 - \varphi_{\text{ES}}}{1 - \sum_{k \in \{\text{ES, HS, Aa}\}} \varphi_k} U_{\text{HES}} \quad (29)$$

The overall benefits of multiple ESSs are shared among the ESS entities based on the average share of regulation costs and FR mileage factors for each storage system. φ_k is the apportionment coefficient of subject k . The specific calculation is as follows:

$$\varphi_k = \left\{ \sum_{t=1}^T \left[\left(\frac{\partial f_k^{\text{FS}}(P_t^k)}{\partial (P_t^k)} + \frac{\partial f_k^{\text{PFR}}(P_t^{k\text{-PFR}})}{\partial (P_t^{k\text{-PFR}})} + \frac{\partial f_k^{\text{PFR}}(P_t^{k\text{-RV}})}{\partial (P_t^{k\text{-RV}})} \right) / f_{\text{all}}' \right] + \frac{\omega_{k\text{-PFR}}}{\sum_{k \in \{\text{ES, HS, Aa}\}} \omega_{k\text{-PFR}}} \right\} / 2 \quad (30)$$

The sum of the unit regulation costs for each type of ESS is denoted as f_{all}' . $\omega_{k\text{-PFR}}$ represents the FR mileage factor for class k 's ESS.

4. Solution of a Two-Level Game Model

A transaction model based on the N–S–C game was proposed in this study. The upper layer is a multitype user demand decision model based on the Nash game, which is solved by the multiobjective whale optimization algorithm (MOWOA). The lower level is a complex, single-objective optimization problem with nonlinear characteristics based on the Nash game for multitype user demand decision mode. It is solved using the improved whale optimization algorithm (IWOA). The two algorithms are both based on the standard whale algorithm, which has simple optimization principles, no control parameters that require empirical setting, and a strong optimization ability. The whale algorithm has been widely used in many large-scale optimization problems and has been verified to be superior to classical intelligent algorithms, such as the particle swarm optimization and the genetic algorithm, in terms of its optimization accuracy and speed after a large number of function tests [21]. However, the standard whale algorithm still has the problem of not effectively balancing global and local search capabilities, resulting in a loss of algorithm diversity and insufficient convergence ability in the later iteration stage. The standard algorithm was improved by proposing IWOA and further proposing MOWOA. The specific explanation of the algorithms can be found in [22].

The solving process of the transaction model based on the Nash–Stackelberg–cooperative game is shown in Figure 2.

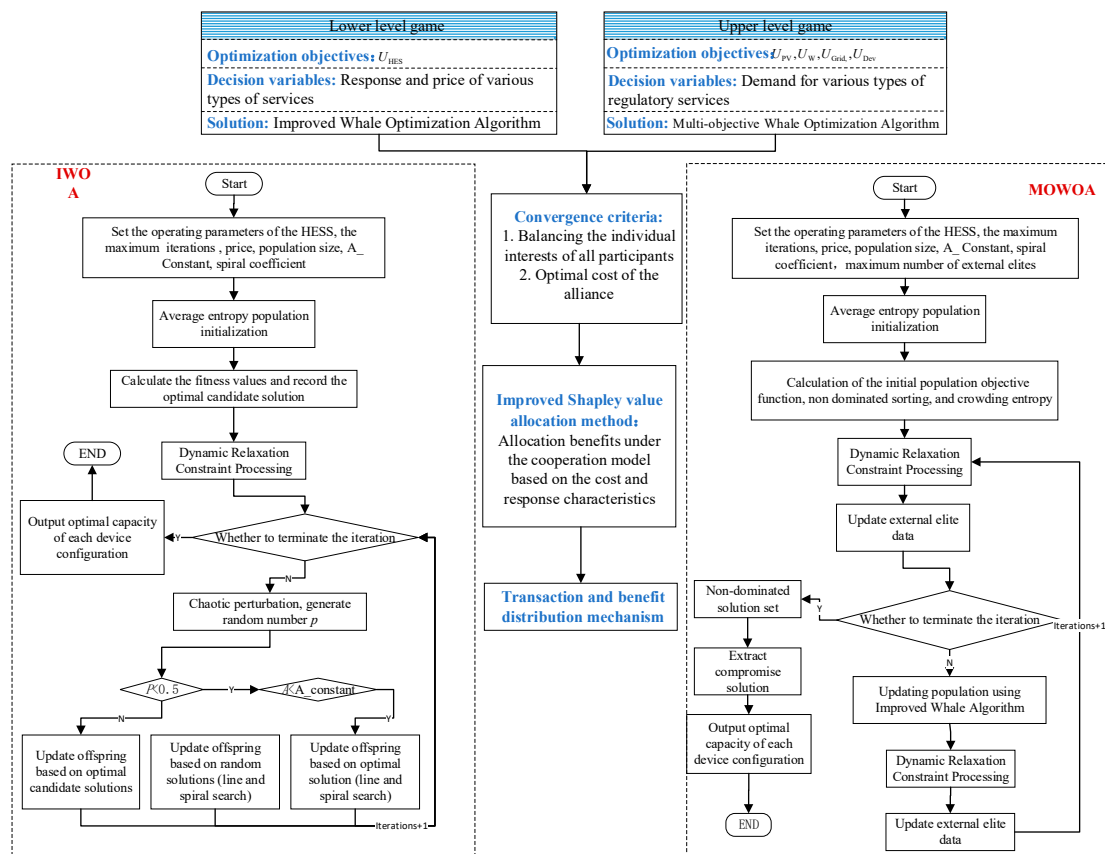
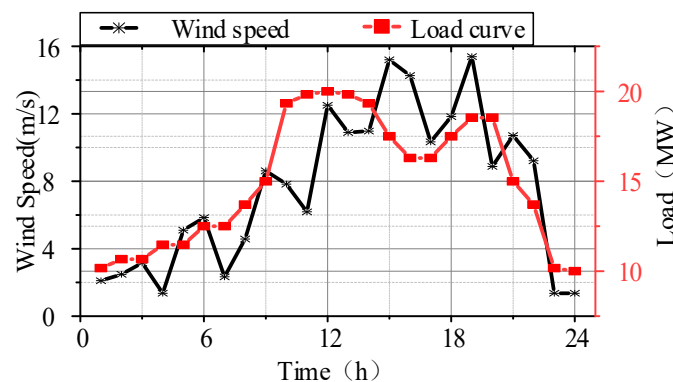


Figure 2. The solution process of the transaction model.

5. Case Study

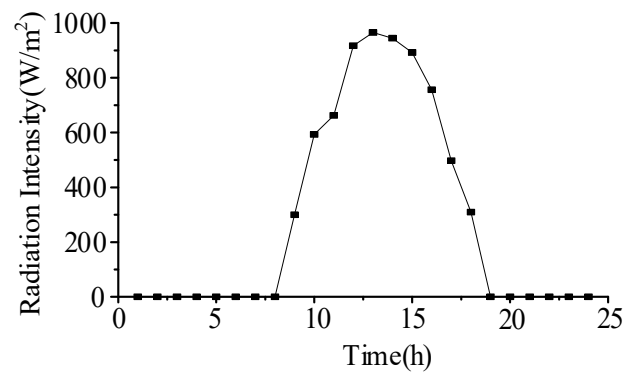
5.1. Basic Parameter

The data from typical days were selected to construct the arithmetic example. The data came from an open economic zone with multiple complementary and comprehensive energy sources, which is located in the Gansu Longdong region in the northwestern part of China. The wind speed and solar irradiation intensity data are shown in Figure 3. The generalizability of the article can be improved by using IEEE 30 as an arithmetic system. The parameters of the three thermal units in the system are shown in Table 1. The system contains the BESS, CAES, and HSS with the parameters shown in Table 2. The variable operating range of the CAES is 0.7 to 1. Wind and photovoltaic RGS are rated at 10 MW. η^{PFR} and η^{RV} of the system are 0.01 and 0.2, respectively.



(a) Wind speed and load curve on a typical day in summer

Figure 3. Cont.



(b) Irradiation intensity on a typical day in summer

Figure 3. Wind speed and irradiance intensity load curves on a typical summer day.**Table 1.** The parameters of thermal units.

Thermal Units	Upper Limit /MWh	Lower Limit /MWh	Climbing Power /MW	Cost Coefficient/¥ (MWh) ⁻¹			
				a ^B	b ^B	a ^{PFR}	a ^{RV}
1	8	3	2	160	1.6	14	12
2	5	2	0.5	140	1.4	12	15
3	5	2	0.5	210	2	16	15

Table 2. The parameters of ESS.

Parameter	Value	Parameter	Value	Parameter	Value	Parameter	Value
SOC _{max} ^{ES} (%)	95	SOC _{min} ^{ES} (%)	15	E _R ^{ES} (MWh)	2	β _{e,j}	1
η ^{ch} (%)	93	η ^{dis} (%)	93	m _{AC,t} (kg/s)	0.4	ω ^{ES_PFR} (%)	50%
P _{max} ^{ES_PFR} (MW)	0.5	Q _{max} ^{ES_RV} (MWh)	1	m _{EX,t} (kg/s)	1.44	ω ^{HS_PFR} (%)	20%
P _{i,max} ^G , P _{i,min} ^G (MW)	1/0	p _{min} st , p _{max} st (MPa)	4 (5.5)	Compressor (expander) efficiency (%)	85	Compressor (expansion) level	4
β _{c,k}	3.5	η _{ele} /η _{fue} (%)	60/95	Q ^{ele} /Q ^{fue} (MW)	2.5/2	P _{max} ^{AC} /P _{max} ^{EX} (MW)	2/1.2
P _{min} ^{AC} /P _{min} ^{EX} (MW) environment temperature (K)	0.8/0.48 298	M _{max} ^{H₂} , M _{min} ^{H₂} (kg)	2800/500	Rated inlet temperature of compressor (K)	312	Rated inlet temperature of expander (K)	363

5.2. Analysis of Joint Bidding Results for Multiple ESSs

Figure 4 shows the trading prices of the demand for standby power, peak shaving, and FR. In Figure 4, the joint peak shaving price of multiple ESSs is positively correlated with the net load curve. The supply and demand of electricity in the region is correctly reflected. The price of electricity market transactions increases significantly with the load growth when the net load is at the peak hours. Fluctuations in peak shaving prices are more pronounced during the time periods, 9–12 and 15–20, because the net load has a high variability, and even some moments of the net load are in the peak period. Thermal units are limited by ramping constraints, leading to higher price incentives for hybrid ESSs. The FR and standby power market are keeping pace with the trend in demand. There are thermal power units and ESS winning bids for each time slot. In the frequency adjustment market, Unit 1 and Unit 2, which have lower cost coefficients, have more winning bids. Similarly, Unit2 has a higher volume of winning bids in the standby power market. In addition, it is easy to see in Figure 4 that the offer at the demand trough is equal to the average of the marginal costs of the FR and standby power for thermal units.

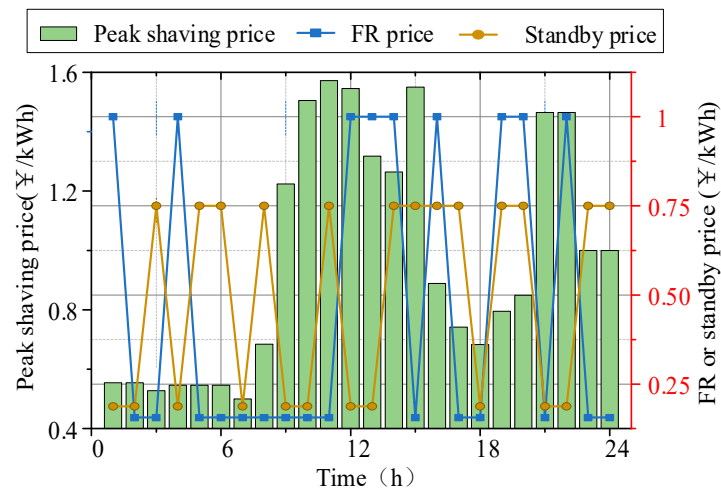


Figure 4. Trading prices for backup, peak shaving, and FR.

The comparison between the peak shaving price and the marginal cost of thermal units is shown in Figure 5a. The ESS does not have a price advantage in the electricity market when the scale of storage is small. The marginal cost reaches the lower boundary of the trading price for the thermal unit, Unit 2, with a larger marginal cost, when the single charging and discharging power of the energy storage exceeds 3 MWh. For Unit 3, the single charging and discharging power of the ESS has to exceed 0.8 MWh in order to reach the lower boundary. The unit subsidy for ESS charging and discharging, shown in Figure 5b, is derived from the average price of 338 ¥/MWh for electricity market transactions. It is easy to see that when the charging/discharging power of the ESS is in the range of 0~20 MWh, the unit subsidy has a tendency to transform as an exponential function with an increase in power. A larger subsidized price per unit is required for power less than 10 MWh, while no additional subsidy is required for power greater than 18 MWh. The results indicate that the allocation capacity of the ESS needs to be upgraded in the future from decentralized storage to independent/shared storage. In this way, the scale effect can be utilized to reduce the investment and operating costs of the ESS.

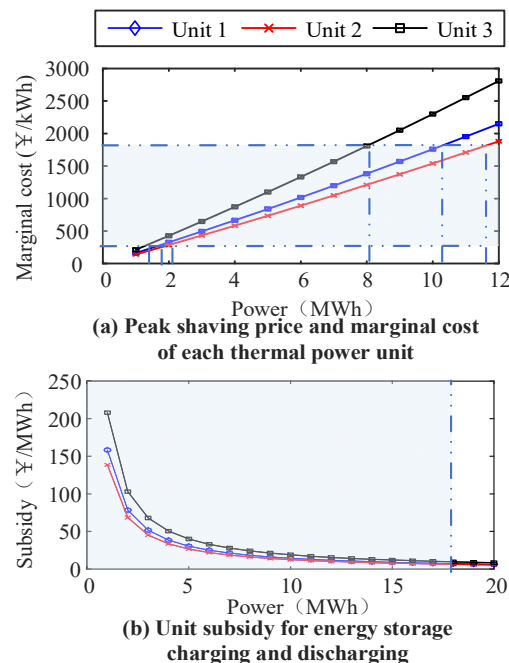


Figure 5. Comparison of peaking shaving price and marginal cost of each thermal power unit.

5.3. Benefit and Utilization Analysis of Multiple ESSs

Table 3 illustrates a comparison of the benefits of multiple ESSs with different levels of market participation. The iterative results of the multiple ESS operator benefits are shown in Figure 6. It is clear that the ESS will receive a higher return by participating in peak shaving, FR, and standby power trading at the same time. ESS operators can recover their investment costs in about 3 to 4 years, if the multiscenario regulation needs of electricity and ancillary services are taken into account. If the ESS is only involved in peak shaving and only considered to meet the demand and supply balance needs of electricity, it will take 5 to 6 years to recover the investment cost.

Table 3. Comparative benefit analysis of energy storage under different market participation.

Case	Participation in Electricity Markets	Participation in FR Market	Participation in Standby Power Market	Multiple ESO Benefits (¥)
Case 1	✓			2.67×10^5
Case 2	✓	✓		2.82×10^5
Case 3	✓		✓	3.95×10^5
Case 4	✓	✓	✓	4.69×10^5

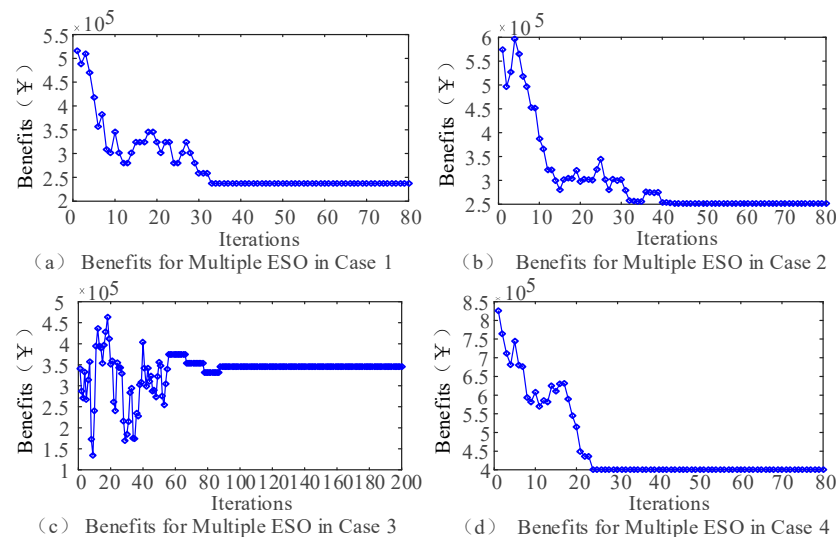


Figure 6. Convergence of energy storage operators' revenue under different market participation.

The degree of utilization of energy storage is defined as:

$$U_{SES} = \sum_{i \in \{ES, HS, Aa\}} \frac{\sum_{t=1}^{24} \left(\frac{|E^i(t) - E^i(t-1)|}{E_{max}^i} \right)}{24} \quad (31)$$

where $E^i(t)$ denotes the equivalent SOC in the hybrid energy storage system. It is estimated that the overall utilization of the hybrid storage is 68.87% when storage is simultaneously involved in peak shaving, frequency regulation, and standby power trading, i.e., Case 4. In addition, the utilization of energy storage increased by 37.3% and 3.2% compared to Case 2 and Case 3, respectively. Because thermal units are limited by operational constraints, such as ramping, the participation of the storage in standby power trading is significant for increased utilization.

Table 4 shows the benefits and overall system benefits of various types of energy storage under different cooperation modes. It is easy to see that the benefits of the BESS are greater in the noncooperative mode than in the cooperative mode. Thus, even if the full cooperation yields the optimal allocation solution for the total investment, the BESS will tend to work individually, driven by individual interests. As a result, the structure of

the alliance under the full cooperation model is broken. The benefit is apportioned using the Shapley value method, improved by Equation (29) for ensuring the stability of the coalition with an optimal overall profit. The comparison of benefits before and after the apportionment of each type of ESS is shown in Figure 7.

Table 4. Benefits analysis of each participant under different cooperation degrees.

Extent of Cooperation	Participants	Benefits of ESS (¥)	Total Profit (¥)
Full cooperation	BESS	180,524	4.69×10^5
	HES	138,727	
	CAES	149,859	
Noncooperation	BESS	182,258	4.16×10^5
	HES	110,825	
	CAES	123,324	

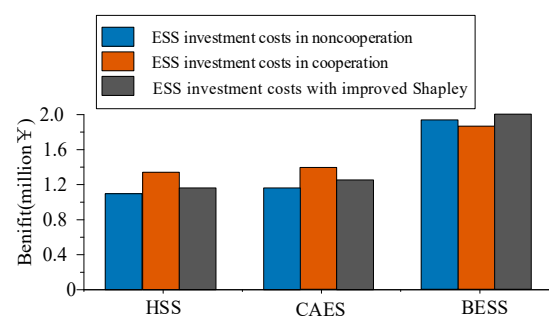


Figure 7. Comparison before and after cost allocation using improved Shapley value.

As indicated by the results in Figure 7 and Table 4, after cost sharing using the improved Shapley value, the cost of the kinds of ESS benefits is less than that in noncooperation. The stability of the alliance in a full cooperation is guaranteed. In addition, the HSS is considered to have a long-time regulation capability and cogeneration characteristics by improving the Shapley value. Therefore, it is possible to take into account the cost of regulation and the FR mileage factor of the ESS for benefit sharing. The interaction of interests of participants with different characteristics for participating in the transaction is rationally reflected.

5.4. Analysis of Trading Influence

The evolution of the RES penetration shapes the transactions in the market, with Figure 8 illustrating the variation of winning bids for the ESS under different wind penetration levels.

By extension, the complementation between the REG and load results in a reduction of net load and a reduction in the system's FR demand following the increasing penetration of the RES. The gap in the trading amount of storage in the FR trading is not large, however, because in conjunction with the transaction prices in Figure 4, the FR power can be used as a spinning reserve capacity in case of surplus and at lower prices. Meanwhile, the RES output randomly increases on account of the increasing penetration level. The system standby demand constantly expands, and under the condition of the priority fulfilment of the declared amount, the winning amount of thermal power units increases accordingly, for which the corresponding utilization rate will show a trend of first increasing and then decreasing, which is presented in Figure 9.

Moreover, as the penetration rate of new energy increases, the demand for energy storage in new energy stations increases, and the profits of energy storage operators correspondingly increase. But, as the penetration rate of new energy continues to increase, more uncertainty will be considered, leading to an increase in risk value. Energy storage faces greater risks, and the revenue of energy storage operators decreases. Therefore, the revenue of energy storage operators also shows a convex trend of increasing first and then decreasing, as shown in Figure 9.

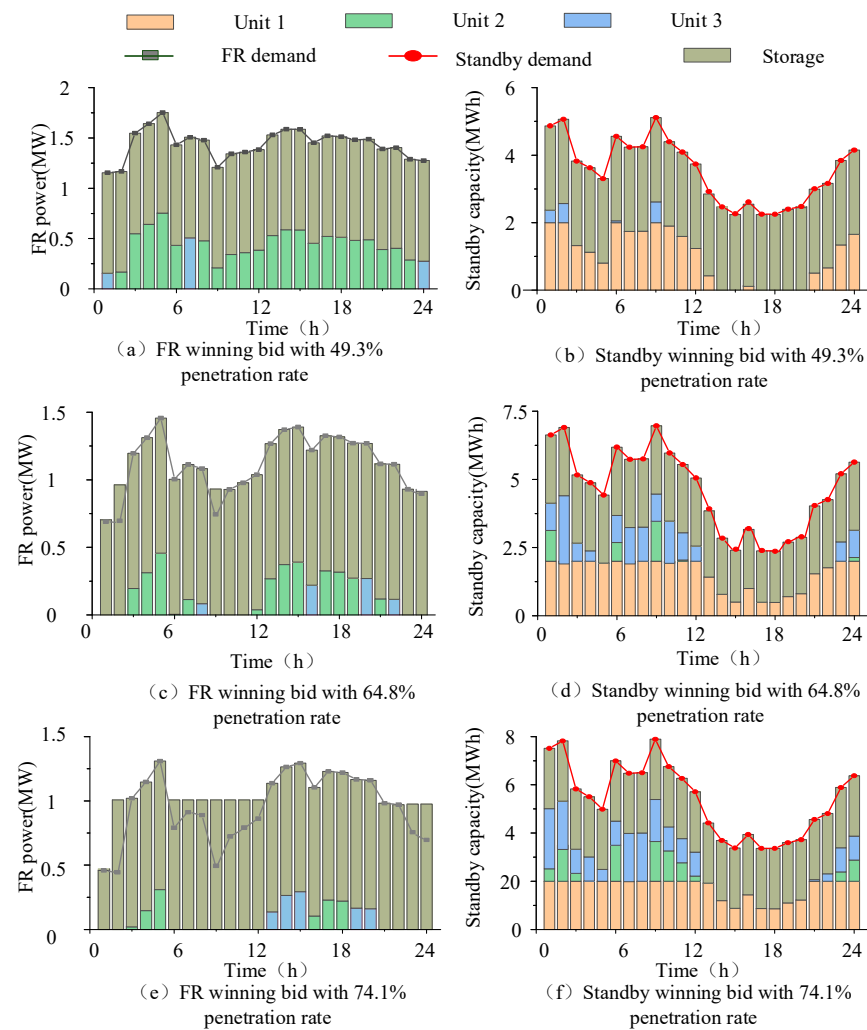


Figure 8. Bids for ESS under different RES permeabilities.

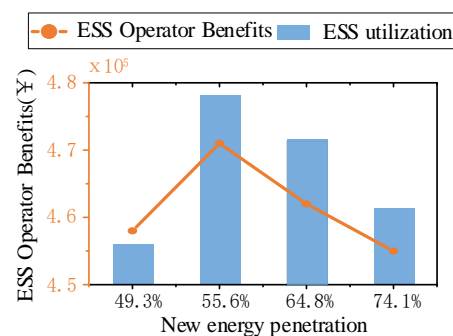


Figure 9. ESS utility and utilization ratio under different permeability.

6. Conclusions

In this study, a day-ahead transaction pattern contemplating the coordination of multiple ESSs was addressed. It tackled the lack of ability for flexible conditions in a high percentage of RESs, promoting the process of China’s electricity marketization reform. The main conclusions were as follows:

- (1) A two-layer game model based on the N–S–C game was constructed. The model balanced the regulating total costs and multiple independent operating profit. The model correctly reflected the supply and demand relationship of the market, surpassing the limitation of poor flexibility caused by insufficient grid-connected synchronous machines.

- (2) A trading pattern for the participation of the ESS in the combined peak-frequency-standby market was designed. The pattern enabled us to boost ESS revenues and utilization and to cut down the payback period. However, a small-scale ESS with a rated power of less than 18 MWh lacked a price advantage, indicating the necessity of upgrading the configuration of the ESS from a decentralized to an independent/shared pattern.
- (3) A comprehensive analysis setting the perspective of a gradual increase in the penetration of the RES was conducted, pointing to the trend of increasing and then decreasing the benefits and utilization of the ESS. Derived from this, the sensitivity parameters had to be rationally selected for ensuring the operation of the system and improving the economy of the system regulation.

In addition, a fair and efficient trading mechanism for the ESS considering heterogeneity will be designed. It can further promote the multiple types of ESSs to meet multiscenario demands and improve their participation in the power market, further contributing to the flexibility and sustainability of the RES.

Author Contributions: Conceptualization, J.Z., Y.X. and L.C.; methodology, X.L.; formal analysis, C.S.; investigation, K.Z. All authors have read and agreed to the published version of the manuscript.

Funding: This research was funded by State Grid Gansu Electric Power Company Technology Project (Research on the Adaptability and Development Strategy of Different Types of New Energy Storage Applications in the Construction of Gansu New Power System), grant number W23FZ2708040" and National Natural Science Foundation of China, grant number U22A20224.

Institutional Review Board Statement: Not applicable.

Informed Consent Statement: Not applicable.

Data Availability Statement: Data are contained within the article.

Conflicts of Interest: The authors declare no conflict of interest.

Nomenclature

$p_t^{W_loss}, p_t^{PV_loss}$	Abandoned wind and solar power at time t	$p_{i,t}^G$	Output of thermal power generator i at time t
$p_t^{RV}, p_t^{PS}, p_t^{PM}$	Standby, peak shaving, and frequency regulation demands for energy storage users at time t	C_k^m, P_k^m	The cost and declared amount of energy storage type K for regulating demand m
$p_t^{RV*}, p_t^{PS*}, p_t^{PFR*}$	Response of energy storage operators to standby, peak shaving, and frequency regulation needs at time t	$\zeta_t^{RV}, \zeta_t^{PS}, \zeta_t^{PFR}$	Trading prices for standby, peak shaving, and frequency modulation needs at time t
U_W, U_{PV}	Benefits of wind and photovoltaic power stations	$\zeta_t^{W_loss}, \zeta_t^{PV_loss}$	Penalty cost for abandoned wind and solar power at time t
$f^B(\cdot), f^{PFR}(\cdot), f^{RV}(\cdot)$	Cost functions for power generation, frequency regulation, and standby of thermal units	$p_{i,t}^G, p_{i,t}^{G_PFR}, Q_{i,t}^{G_RV}$	The planned output, frequency regulation and standby of thermal power generation unit i used for output and at time t
U_{Grid}	Grid benefits	U_{Dev}	Feedback deviation
$\zeta_{Dev}^{PS}, \zeta_{Dev}^{PFR}, \zeta_{Dev}^{RV}$	Feedback deviation factor	D_t	Predicted load at time t

P_t^W, P_t^{PV}	Predicting wind power and photovoltaic output at time t	$P_{i,max}^G, P_{i,min}^G$	Upper and lower limits of output for thermal unit i
P_i^{RU}, P_i^{RD}	Up and down climbing rates of thermal power generator i	U_{HES}	Benefits of hybrid energy storage systems
$P_t^{ES_C}, P_t^{ES_D}$	Charging and discharging power of electrochemical energy storage at time t	P_t^{ele}, P_t^{fue}	The power of electrolytic cells and fuel cells at time t
P_t^{AC}, P_t^{EX}	The power of the air compressor and expander at time t	$P_t^{ES_PFR}, P_t^{HS_PFR}, P_t^{Aa_PFR}$	Declared power of each type of entities participating in primary frequency regulation at time t
$Q_t^{ES_RV}, Q_t^{Aa_RV}, Q_t^{HS_RV}$	The declared standby capacity of multiple entities at time t	μ_t^C, μ_t^D	The charging and discharging state of electrochemical energy storage at time t
$P_{max}^{ES_C}, P_{max}^{ES_D}$	Maximum charging and discharging power of energy storage	$\omega^{ES_PFR}, \omega^{ES_RV}$	Factors involved in frequency regulation and standby of electrochemical energy storage
$E_{min}^{ES}, E_{max}^{ES}$	Upper and lower limits of electrochemical energy storage capacity	η^{ch}, η^{dis}	Charging and discharging efficiency of electrochemical energy storage
$M_t^{H_2}, M_{max}^{H_2}, M_{min}^{H_2}$	Gas in the hydrogen storage tank at time t and its upper and lower bounds	η_{ele}, η_{fue}	Energy conversion efficiency of electrolytic cells and fuel cells
$P_t^{st}, P_{min}^{st}, P_{max}^{st}$	Air pressure and its upper and lower limits in the storage chamber at time t	V_{st}	Air storage chamber volume
$\dot{m}_{AC,t}, \dot{m}_{EX,t}$	Air mass flow rates into out of the expander at time t	$T_{st,in}, T_{st}$	The temperature at the air inlet and inside the storage chamber
R_g, γ	Ideal gas constant and specific heat capacity	η_{AC}, η_{EX}	Operating efficiency of compressors and expanders
$T_{c,k,in}, T_{c,n,in}$	Ideal air temperature at the inlet of the k stage and final stage compressors	$\beta_{c,k}, \beta_{c,n,t}$	The compression ratio of the k stage and the final stage compressor under rated operating conditions at time t
n	Number of compressor and expander stages	$T_{e,j,in}$	Ideal air temperature at the inlet of the j stage expander
$\beta_{e,j}$	Expansion ratio of j level expander under rated operating state	μ_t^{AC}, μ_t^{EX}	Operating state variables of compressor and expander at time t
T_{on}^{AC}, T_{on}^{EX}	Minimum working time for compressors and expanders	ω^{HS_PFR}	Factors of hydrogen energy storage participating in frequency modulation mileage

References

1. Ding, T.; Sun, J.; Huang, Y.; Mu, C.; Huang, W.; Geng, S. Domestic and Foreign Present Situation of Capacity Market with Energy Storage and Thought on Its Mechanism. *Autom. Electr. Power Syst.* **2023**, 1–22.
2. Xie, X.; Ma, N.; Liu, W.; Zhao, W.; Xu, P.; Li, H. Functions of Energy Storage in Renewable Energy Dominated Power Systems: Review and Prospect. In Proceedings of the CSEE, Lisbon, Portugal, 29–31 March 2023; Volume 43, pp. 158–169.
3. Chen, X. Research on the Development Problems and Countermeasures of Electrochemical Energy Storage Industry in China. *Energy Res. Util.* **2023**, *15*, 39–42.
4. National Development and Reform Commission. Notice on Further Promoting the Participation of New Energy Storage in the Electricity Market and Dispatching Application. *Bull. State Counc. People's Repub. China* **2022**, 475.
5. Ahmadi, S.E.; Sadeghi, D.; Marzband, M.; Abusorrah, A.; Sedraoui, K. Decentralized bi-level stochastic optimization approach for multi-agent multi-energy networked micro-grids with multi-energy storage technologies. *Energy* **2022**, *245*, 123223. [[CrossRef](#)]
6. Cheng, S.; Wang, R.; Xu, J.; Wei, Z. Multi-time scale coordinated optimization of an energy hub in the integrated energy system with multi-type energy storage systems. *Sustain. Energy Technol. Assess.* **2021**, *47*, 101327. [[CrossRef](#)]
7. Liu, Y.; Liu, Q.; Guan, H.; Li, X.; Bi, D.; Guo, Y.; Sun, H. Optimization strategy of configuration and scheduling for user-side energy storage. *Electronics* **2021**, *11*, 120. [[CrossRef](#)]
8. Okubo, T.; Shimizu, T.; Hasegawa, K.; Kikuchi, Y.; Manzhos, S.; Ihara, M. Factors affecting the techno-economic and environmental performance of on-grid distributed hydrogen energy storage systems with solar panels. *Energy* **2023**, *269*, 126736. [[CrossRef](#)]
9. Anthony, M.G.; Xiao-Yu, W. Hybrid lithium-ion battery and hydrogen energy storage systems for a wind-supplied microgrid. *Appl. Energy* **2023**, *345*, 121311.
10. Yan, H.; Zhang, W.; Kang, J.; Yuan, T. The necessity and feasibility of hydrogen storage for large-scale, long-term energy storage in the new power system in china. *Energies* **2023**, *16*, 4837. [[CrossRef](#)]
11. Deng, J.; Wang, X.; Chen, T.; Meng, F. An energy router based on multi-hybrid energy storage system with energy coordinated management strategy in island operation mode. *Renew. Energy* **2023**, *212*, 274–284. [[CrossRef](#)]
12. Cui, S.; Wu, J.; Gao, Y.; Zhu, R. A high altitude prosumer energy cooperation framework considering composite energy storage sharing and electric-oxygen-hydrogen flexible supply. *Appl. Energy* **2023**, *349*, 121601. [[CrossRef](#)]
13. Pan, C.; Fan, H.; Zhang, R.; Sun, J.; Wang, Y.; Sun, Y. An improved multi-timescale coordinated control strategy for an integrated energy system with a hybrid energy storage system. *Appl. Energy* **2023**, *343*, S0306261923005019. [[CrossRef](#)]
14. Jiang, Y.; Kang, L.; Liu, Y. Multi-objective design optimization of a multi-type battery energy storage in photovoltaic systems. *J. Energy Storage* **2021**, *39*, 102604. [[CrossRef](#)]
15. Lai, S.; Qiu, J.; Tao, Y. Credit-based pricing and planning strategies for hydrogen and electricity energy storage sharing. *IEEE Trans. Sustain. Energy* **2022**, *13*, 67–80. [[CrossRef](#)]
16. Hemmati, R.; Mehrjerdi, H.; Bornapour, M. Hybrid hydrogen-battery storage to smooth solar energy volatility and energy arbitrage considering uncertain electrical-thermal loads. *Renew. Energy* **2020**, *154*, 1180–1187. [[CrossRef](#)]
17. Li, X.; Chen, L.; Du, X.; Wen, J. Research Status and Prospect of Shared Energy Storage Operation Mechanism and Trading Mode on Generation Side. *J. Electr. Eng.* **2023**, *18*, 188–200.
18. An, Q.; Wang, J.; Wu, Z.; Zhong, H.; Li, G. Benefit allocation mechanism design of electricity markets with penetration of high proportion of renewable energy. *Autom. Electr. Power Syst.* **2022**, *46*, 13–22.
19. Xing, S.; Xie, J.; Jin, Y.; Zhou, C. Agent-based simulation of day-ahead market pricing mechanism for energy-frequency regulation-reserve combined operation for power systems with wind power. *Power Syst. Technol.* **2022**, *12*, 1–12.
20. Fan, T.Y.; Wang, H.Y.; Wang, W.Q. Coordinated optimization scheduling of microgrid and distribution network based on cooperative game considering active/passive demand response. *Power Syst. Technol.* **2022**, *46*, 453–463.
21. Seyedali, M.; Lewis, A. The Whale Optimization Algorithm. *Adv. Eng. Softw.* **2016**, *95*, 51–67.
22. Li, X.; Wang, W. Bi-level robust game optimal scheduling of regional comprehensive energy system. *J. Zhejiang Univ. Eng. Sci.* **2021**, *55*, 177–188.

Disclaimer/Publisher's Note: The statements, opinions and data contained in all publications are solely those of the individual author(s) and contributor(s) and not of MDPI and/or the editor(s). MDPI and/or the editor(s) disclaim responsibility for any injury to people or property resulting from any ideas, methods, instructions or products referred to in the content.